View metadata, citation and similar papers at core.ac.uk

brought to you by CORE

provided by Digital.CSIC

The Journal of Chemical Physics

A five-dimensional potential-energy surface for the rotational excitation of SO_2 by H_2 at low temperatures

Cite as: J. Chem. Phys. **131**, 014305 (2009); https://doi.org/10.1063/1.3158357
Submitted: 26 March 2009 . Accepted: 03 June 2009 . Published Online: 07 July 2009

A. Spielfiedel, M.-L. Senent, F. Dayou, C. Balança, L. Cressiot-Vincent, A. Faure, L. Wiesenfeld, and N. Feautrier


View Online


Export Citation

ARTICLES YOU MAY BE INTERESTED IN

R12-calibrated H_2O-H_2 interaction: Full dimensional and vibrationally averaged potential energy surfaces
The Journal of Chemical Physics **129**, 134306 (2008); https://doi.org/10.1063/1.2988314

Theoretical study of the rovibrational spectrum of H_2O–H_2
The Journal of Chemical Physics **134**, 044313 (2011); https://doi.org/10.1063/1.3533230

A full nine-dimensional potential-energy surface for hydrogen molecule-water collisions
The Journal of Chemical Physics **122**, 221102 (2005); https://doi.org/10.1063/1.1935515

Lock-in Amplifiers up to 600 MHz
Watch

AIP Publishing

© 2009 American Institute of Physics.

A five-dimensional potential-energy surface for the rotational excitation of SO_2 by H_2 at low temperatures

A. Spielfiedel,[1,a)] M.-L. Senent,[2] F. Dayou,[1] C. Balança,[1] L. Cressiot-Vincent,[1,2] A. Faure,[3] L. Wiesenfeld,[3] and N. Feautrier[1]
[1]*Laboratoire d'Etude du Rayonnement et de la Matière, Observatoire de Paris-Meudon, CNRS UMR 8112, 5 Place Jules Janssen, 92195 Meudon Cedex, France*
[2]*DAMIR, Instituto de Estructura de la Materia, CSIC, C/Serrano 121, 28006 Madrid, Spain*
[3]*Laboratoire d'Astrophysique, Observatoire de Grenoble (LAOG), Université Joseph Fourier, CNRS UMR 5571, B.P. 53, 38041 Grenoble Cedex 09, France*

(Received 26 March 2009; accepted 3 June 2009; published online 7 July 2009)

The SO_2 molecule is detected in a large variety of astronomical objects, notably molecular clouds and star-forming regions. An accurate modeling of the observations needs a very good knowledge of the collisional excitation rates with H_2 because of competition between collisional and radiative processes that excite and quench the different rotational levels of SO_2. We report here a five-dimensional, rigid-body, interaction potential for SO_2-H_2. As a first application, we present rate constants for excitation/de-excitation of the 31 first levels of SO_2 by para-H_2 at low temperatures. Propensity rules are discussed. © *2009 American Institute of Physics*.
[DOI: 10.1063/1.3158357]

I. INTRODUCTION

From its first detection in interstellar space in 1975,[1] SO_2 has been detected in a great variety of astronomical objects. SO_2 is an abundant species in warm molecular clouds and in circumstellar envelopes of evolved stars. It has also been detected in dark and cold clouds.[2] A detailed study[3] of the L134N dark cloud from observations of emission of various molecules including SO_2 shows large abundance variations of this species, according to the position in the cloud. However, such study in terms of physical and chemical conditions is based on statistical equilibrium calculations where collisional coefficients and radiative rates come from previously published data. By taking into account the sensitivity of the radiative transfer models to the collisional rate coefficients and their accuracy on the interpretation of observed spectra,[4–6] it is of a great importance to provide accurate collisional excitation cross sections with para- and ortho-H_2 for most of the interstellar molecules. Until now, the only available rate coefficients of SO_2 were those computed by Green[7] for collisions with He multiplied by 1.39 to correct for the velocity difference between H_2 and He. Moreover, these excitation rates were calculated within the infinite order sudden approximation (IOS) scattering approach based on a rather approximate potential-energy surface (PES). Even though, several recent papers[8–10] show that rate coefficients for heavy molecules in collision with para-$H_2(J_2=0)$ and He are of the same order of magnitude, with correcting factors between 0.3 and 3, but with no systematic trends. This is insufficient for an accurate modeling, especially at low temperatures when low-energy resonances contribute to the rate coefficients.

A very good knowledge of state-to-state collisional excitation rates requires first an accurate description of the SO_2-H_2 interaction given by the PES. In the present study, we have computed a five-dimensional PES allowing for all the relative orientations of the two collision partners. Then, cross sections and rate coefficients for temperatures up to 30 K were calculated in a full close-coupling approach and collisional propensity rules are investigated. A comparison of the para-$H_2(J_2=0)$ rate coefficients with the previous results for He obtained by Green[7] is presented for $T=25$ K.

The paper is organized as follows. Section II describes details of the PES calculations. The scattering calculations are presented in Sec. III; rate coefficients for collisions with para-H_2 are given in Sec. IV, and conclusions are drawn in Sec. V. The following units are used: bond lengths and distances in Bohr, angles in degrees, energies in cm^{-1}, cross sections in $Å^2$, and rate coefficients in $cm^3\ s^{-1}$.

II. PES

A. Computational strategy

For rotational excitation at energies lower than the threshold for excitation of the vibrational modes of SO_2, the collision partners may be approximated to be rigid, in order to keep the number of degrees of freedom as small as possible. Previous studies have suggested that properly averaged molecular geometries provide a good approximation of the PES averaged over vibration.[11–13] Accordingly, we used the H_2 bond separation $r_{HH}=1.449$ bohrs obtained by averaging over the ground-state vibrational wave function. For SO_2, as vibrational wave functions are not available, we used the molecular constants of Lovas.[14] The bond length is $r_{SO}=2.706$ bohrs and the $O\hat{S}O$ angle is 119.5°.

We used the conventions of Phillips *et al.*[15] in defining the SO_2-H_2 intermolecular potential. As illustrated in Fig. 1,

a)Author to whom correspondence should be addressed. Electronic mail: annie.spielfiedel@obspm.fr.

 © 2009 American Institute of Physics

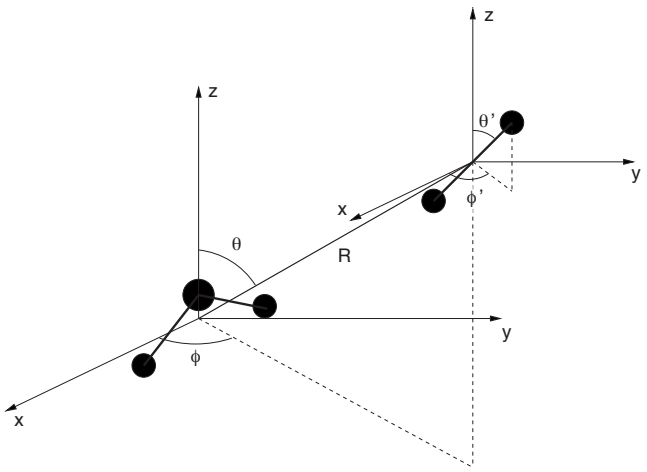

FIG. 1. Five-dimensional body-fixed coordinate system used to describe the interaction between SO_2 and H_2. The SO_2 molecule lies in the xz plane. The orientation of the collision coordinate **R** and the orientation of H_2 are both described with respect to the SO_2-fixed axes by the polar angles (θ,ϕ) and (θ',ϕ'), respectively.

the rigid-body PES involves five coordinates: The collision coordinate $\vec{R}$, i.e., the vector from SO_2 center of mass to H_2 center of mass, described by the spherical polar coordinates (R,θ,ϕ), where R is the radial distance, θ is measured from the z axis and ϕ is measured from the xz plane, and the (θ',ϕ') angles that describe the H_2 orientation relative to the SO_2 molecule in the body-fixed system.

In terms of these relative coordinates, the intermolecular potential can be written as[13,15]

$$V(R,\theta,\phi,\theta',\phi') = \sum_{l_1 m_1 l_2 l} v_{l_1 m_1 l_2 l}(R)\bar{t}_{l_1 m_1 l_2 l}(\theta,\phi,\theta',\phi'), \tag{1}$$

where $\bar{t}_{l_1 m_1 l_2 l}(\theta,\phi,\theta',\phi')$ is the normalized spherical tensor,

$$\bar{t}_{l_1 m_1 l_2 l}(\theta,\phi,\theta',\phi') = \alpha_{l_1 m_1 l_2 l}(1+\delta_{m_1 0})^{-1}\sum_{r_1 r_2}\begin{pmatrix} l_1 & l_2 & l \\ r_1 & r_2 & r \end{pmatrix} Y_{l_2 r_2}(\theta',\phi')Y_{lr}(\theta,\phi) \times[\delta_{m_1 r_1} + (-1)^{l_1+m_1+l_2+l}\delta_{-m_1 r_1}], \tag{2}$$

with the normalization factor[13]

$$\alpha_{l_1 m_1 l_2 l} = [2(1+\delta_{m_1 0})^{-1}(2l_1+1)^{-1}]^{-1/2}. \tag{3}$$

In this expansion, the homonuclear symmetry of H_2 constrains l_2 to be even. The C_{2v} symmetry of SO_2 further requires that m_1 be even. The additional requirements that the potential is invariant with respect to the inversion of all coordinates through the origin (parity invariance) also restrict the sum l_1+l_2+l to even integers. However, it has been demonstrated,[16] by providing counterexamples, that this restriction is actually not required by fundamental spatial symmetry. It was also shown numerically, in the case of H_2O-H_2[13], that functions with l_1+l_2+l odd are small but not negligible. These functions were consequently included in the present study.

We used a supermolecular approach for all the interaction energy calculations. Calculations were performed at the CCSD(T) level[17,18] with seven frozen core orbitals, using the MOLPRO 2006 package.[19] The resulting energies $E_{SO_2-H_2}$ were corrected from the basis set superposition error following the usual counterpoise correction method[20] [Eq. (4)], where E_{SO_2} and E_{H_2} are the energies of the SO_2 and H_2 subsystems, respectively, computed with the full SO_2-H_2 basis set,

$$V(R,\theta,\phi,\theta',\phi') = E_{SO_2-H_2}(R,\theta,\phi,\theta',\phi') - E_{SO_2}(R,\theta,\phi,\theta',\phi') - E_{H_2}(R,\theta,\phi,\theta',\phi'). \tag{4}$$

Converged results were obtained for the radial R grid including 37 regularly spaced distances between 3.50 and 12.50 bohrs, seven regularly spaced distances between 13.0 and 16.00 bohrs, and five points at 17.00, 18.00, 20.00, 25.00, and 30.00 bohrs. The grid points for the angular coordinates of H_2 relative to SO_2 were chosen for each intermolecular distance R via random sampling.[13]

Following a strategy developed for the H_2O-H_2 system,[13] the SO_2-H_2 PES is computed using a three step procedure with set of *ab initio* calculations denoted by "r," "d,"and "t."

(1) The r set provides a reference surface (V^{ref}) calculated from a large number of medium accuracy calculations using the aug-cc-pVDZ basis set of Woon and Dunning[21] and bond functions of William *et al.*[22] placed according to[23]

$$R_b = R + 0.5\frac{\sum_{ij}(w_{ij}r_{ij})}{\sum_{ij}(w_{ij})}, \tag{5}$$

where $w_{ij}=r_{ij}^{-6}$ with $r_{ij}=R_j-R_i$. R is the distance between the centers of mass of SO_2 and H_2, R_i denotes the position of the H_i atom $(i=1,2)$, and R_j denotes the position of each atom j in SO_2.

(2) The d set provides a surface denoted V^d calculated from a smaller number of angular geometries with the same aug-cc-pVDZ basis set and bond functions of William *et al.*[22] located at the center of gravity of the two collision partners to minimize steric hindrance of H_2 by SO_2 at small distances. The new position of the bond functions is given by

$$R_b = 0.5\frac{\sum_{ij} w_{ij}(R_i+R_j)}{\sum_{ij}(w_{ij})}. \tag{6}$$

(3) The t set provides a surface denoted V^t calculated using the more accurate aug-cc-pVTZ basis set[21] augmented by the bond functions of William *et al.*[22] placed at the same positions as in the d set.

This strategy of splitting the calculations into several levels of accuracy was made necessary by the large computational resources required by aVTZ calculations.

TABLE I. Geometries corresponding to absolute and secondary minima with the corresponding distances and angles R, $\theta, \phi, \theta', \phi'$.

N^0	R	θ	ϕ	θ'	ϕ'	V
1	6.15	91.72	90.0	90.0	0.0	−192.723 758
2	6.37	80.89	90.0	0.0	0.0	−161.762 525
3	6.90	180.00	0.0	0.0	0.0	−115.858 191
4	7.11	49.77	0.0	5.69	180.0	−165.170 462
5	7.16	51.65	0.0	0.0	0.0	−164.723 207
6	7.36	154.89	0.0	0.0	0.0	−142.516 177
7	7.77	0.0	0.0	90.0	0.0	−78.338 699
8	8.01	134.02	0.0	143.13	0.0	−146.597 026

B. CCSD(T) PES and global fit

The PES was expanded in terms of a complete orthogonal set of angular functions for any intermolecular distance R [see Eq. (1)]. To obtain convergence of this expansion (see below), we have performed extensive calculations comprising, for each of the 49 intermolecular distances, 8074 random angles for the r set and 520 and 500 sets of angles for the d and t sets, respectively. For set r which provides a reference PES, V^{ref}, the large number of calculated geometries permits to converge the angular expansion to an excellent accuracy at all distances. Sets r, d, and t contain 500 common geometries, whose corresponding energies are used to improve the accuracy of the reference PES. From d and t sets, a complete basis set (CBS) extrapolation of the interaction was performed leading to a new surface denoted "dt." For this extrapolation, the SCF contribution is taken from the t set and is not extrapolated. The correlation contribution was extrapolated as $1/x^3$, where $x=2,3$ for aVDZ and aVTZ basis sets, respectively. The "d-r" energy differences provide a correction for the bond function positions which are better localized in d calculations as the formula respects the symmetry between the two molecules. The results show that this correction is significantly smaller (an order of magnitude) than the CBS correction. The global "dt-r" PES correction is also expected to be less anisotropic than the reference PES. This point, which was verified *a posteriori*, permits to achieve a fair convergence of the corresponding angular expansion of the PES correction (denoted δ^{corr}) with 500 geometries only. To summarize, the final intermolecular potential can be written as

$$V = V^{\text{ref}} + \delta^{\text{corr}}. \tag{7}$$

Preliminary tests of fitting the SO_2–H_2 interaction over the angular expansion Eq. (1) had shown difficulties owing to the large (short-range) anisotropy of this system. Similar although more severe steric hindrance problems had been encountered previously for the HC_3N–H_2 system.[9] For this latter system, an original and successful solution was proposed by Wernli *et al.*[9] Following these authors, we have thus regularized the SO_2–H_2 PES by introducing a scaling function S_f. For intermolecular distances $R \leq 11\ a_0$, the interaction V was thus replaced by $S_f(V)$, which returns V when V is lower than a prescribed threshold (see below), and then smoothly saturates to a limiting value when V grows up into the repulsive walls. Consequently, the regularized PES retains only the low-energy content of the original PES, unmodified up to the range of the threshold energy. In contrast to the original PES, it can be easily expanded over Eq. (1) to an excellent accuracy and is thus well adapted to quantum close-coupling studies. We have selected a threshold value of 10 000 cm^{-1}, high enough for applications where both molecules can be kept rigid.

The above regularization procedure was applied to both V^{ref} and δ^{corr} PES. At each intermolecular distance, these regularized PESs were then developed over the angular expansion (1) using a standard linear least-squares fit procedure. We selected a maximal order which includes all anisotropies up to $l_1=16$ for SO_2 and $l_2=4$ for H_2, resulting in 1094 $\bar{t}_{l_1 m_1 l_2 l}$ functions. We then selected iteratively all statistically significant terms using the following procedure (at each intermolecular separation): We started the fit with a minimal expansion limited to the single $\bar{t}_{0000}$ function and evaluated the 1093 remaining terms by a Gauss quadrature; all terms above a threshold parameter (see details in Valiron *et al.*[13]) were then selected and added to $\bar{t}_{0000}$, providing a new starting expansion. The process was reiterated until convergence. In the case of the reference PES V^{ref}, the final set, obtained by merging the selected sets at all distances, was composed of 129 angular functions, including anisotropies up to $l_1=13$ for SO_2 and $l_2=4$ for H_2. In the case of the dt-r PES correction δ^{corr}, the final set was composed of 47 angular functions (a subset of the above 129 functions), including anisotropies up to $l_1=11$ for SO_2 and $l_2=4$ for H_2. As expected, the dt-r PES correction was found to be much less anisotropic than the reference surface. Both sets were used for all 49 intermolecular distances. The accuracy of the angular fitting procedure was estimated from the root-mean-square residual which was found both for V^{ref} and δ^{corr} to be lower than 1 cm^{-1} for R larger than $6.5a_0$. This result indicates the high quality of the angular fit in the long range and van der Waals minimum regions of the interaction.

The PES exhibits various minima which were found using a quasi-Newton algorithm. The global minimum was found to be $V_{\text{min}}=-192.723\ 758\ \text{cm}^{-1}$ for $R=6.147\ 979$ bohrs, $\theta=91.721\ 778°$, $\phi=90.0°$, $\theta'=90.0°$, and $\phi'=0°$. Seven secondary minima were also found (some of them should be duplicated by symmetry), their coordinates are given in Table I. Figure 2 presents contour plots of the PES: In this graph, the SO_2 molecule stands in the xz plane

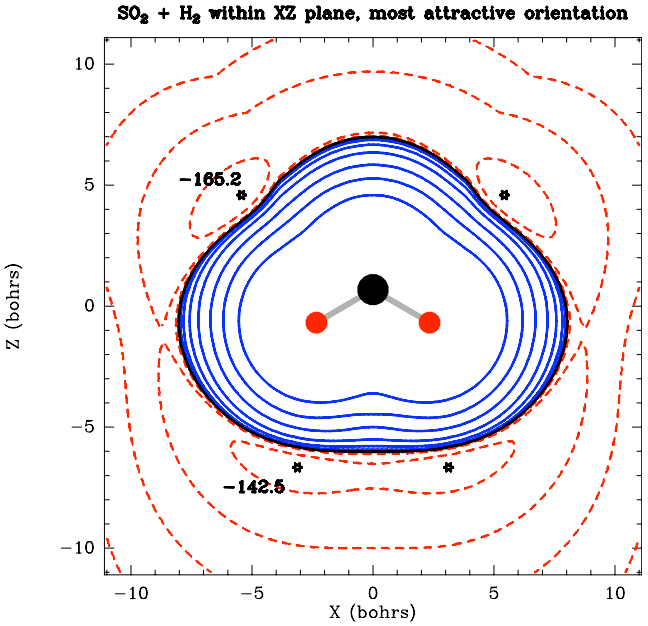

FIG. 2. Contour plot of the SO_2-H_2 PES with H_2 in the xz plane. The SO_2 molecule is shown to scale. Equipotentials (in cm^{-1}): dashed lines: −3, −10, −30, −100; fat bold line: 0; solid lines: 3, 10, 30, 100, 300, 1000, 3000, 10 000.

and the H_2 molecule is located in the xz plane. As shown in this figure, the PES exhibits a complicated shape and a strong anisotropy.

It is interesting to analyze the terms of the angular expansion of the PES. Taking as example the expansion for $R=7.0$ bohrs (near the minimum of the isotropic term), one may observe (see Table II) that, except the isotropic term (0000), the dominant terms are the (2202) and (3003) terms that are not excluded for collisions with para-$H_2(J_2=0)$. The dipole-quadrupole (1023) and quadrupole-quadrupole (2224) terms, that are excluded for collisions with para-$H_2(J_2=0)$, are large but not dominant. This contrasts with the situation encountered for H_2O-H_2 collisions (see Table III) where the dominant terms for $R=6.5$ bohrs (minimum of the isotropic term) are the dipole-quadrupole and the quadrupole-quadrupole. One can thus expect smaller H_2 ortho-para differences in the cross sections for SO_2 than those obtained for H_2O.[24] We can also expect a small effect of including the $J_2=2$ state in the para-H_2 basis set (see below).

III. SCATTERING CALCULATIONS

In the following J, J' denote the rotational angular momentum of SO_2 and J_2 denotes the rotational angular momentum of H_2. We performed extensive calculations of cross sections for collisions of SO_2 (^{16}O isotope) with para-$H_2(J_2=0)$ at low energies.

Close-coupling calculations were performed with the mixed MPI and OpenMP extension[25] of the MOLSCAT V14 package.[26] The asymmetric top wave functions of $^{32}SO_2$ were obtained from the rotational constants and distorsion constants given by Lovas[14] evaluated in the same coordinate system used to describe the PES.[7] The rotational constants about the x, y, and z axes are 2.027 354, 0.293 53, and 0.344 170 cm^{-1}, and the relative distorsion constants are $7.223\,564\times10^{-7}$, $3.355\,084\times10^{-6}$ and $1.026\,74\,2\times10^{-5}$, respectively. For $^{32}SO_2-H_2$ the reduced mass is 1.9 540 708 amu. The symmetry axis (z-axis) corresponds, in standard

TABLE II. Dominant expansion terms (in cm^{-1}) of the SO_2-H_2 PES, $R=7.0$ bohrs.

l_1	m_1	l_2	l	$v_{l_1m_1l_2l}$
0	0	0	0	84.409 983
1	0	0	1	308.920 925
1	0	2	3	−327.300 101
2	0	0	2	−475.069 241
2	2	0	2	1351.683 265
2	2	2	4	−386.426 641
3	0	0	3	−526.467 648

TABLE III. Dominant expansion terms (in cm^{-1}) of the H_2O-H_2 PES, $R=6.5$ bohrs.

l_1	m_1	l_2	l	$v_{l_1m_1l_2l}$
0	0	0	0	−747.753 424
1	0	2	3	544.231 594
2	2	0	2	−99.550 994
2	2	2	4	415.553 651
3	2	2	5	141.418 027

TABLE IV. SO_2 calculated energy levels (in cm^{-1}) compared to values deduced from the JPL molecular spectroscopy catalog (Ref. 27).

Level	J_{K_a,K_c}	This work	JPL
1	$0_{0,0}$	0.0000	0.0000
2	$2_{0,2}$	1. 9118	1.9120
3	$1_{1,1}$	2. 3209	2.3208
4	$2_{1,1}$	3.6973	3.6975
5	$3_{1,3}$	5.3820	5.3820
6	$4_{0,4}$	6.3585	6.3601
7	$4_{1,3}$	8.3327	8.3356
8	$2_{2,0}$	8.7482	8.7469
9	$3_{2,2}$	10.6600	10.6590
10	$5_{1,5}$	10.8856	10.8864
11	$4_{2,2}$	13.2254	13.2258
12	$6_{0,6}$	13.3070	13.3134
13	$6_{1,5}$	15.6009	15.6140
14	$5_{2,4}$	16.3935	16.3950
15	$7_{1,7}$	18.8219	18.8247
16	$3_{3,1}$	19.2034	19.1968
17	$6_{2,4}$	20.2858	20.2941
18	$4_{3,1}$	21.7560	21.7502
19	$8_{0,8}$	22.7113	22.7267
20	$7_{2,6}$	24.6619	24.6713
21	$5_{3,3}$	24.9465	24.9425
22	$8_{1,7}$	25.4805	25.5183
23	$6_{3,3}$	28.7763	28.7760
24	$9_{1,9}$	29.1782	29.1848
25	$8_{2,6}$	29.9571	29.9882
26	$7_{3,5}$	33.2419	33.2472
27	$4_{4,0}$	33.7139	33.6930
28	$10_{0,10}$	34.5216	34.5495
29	$9_{2,8}$	35.4513	35.4777
30	$5_{4,2}$	36.9041	36.8845
31	$10_{1,9}$	37.9416	38.0265

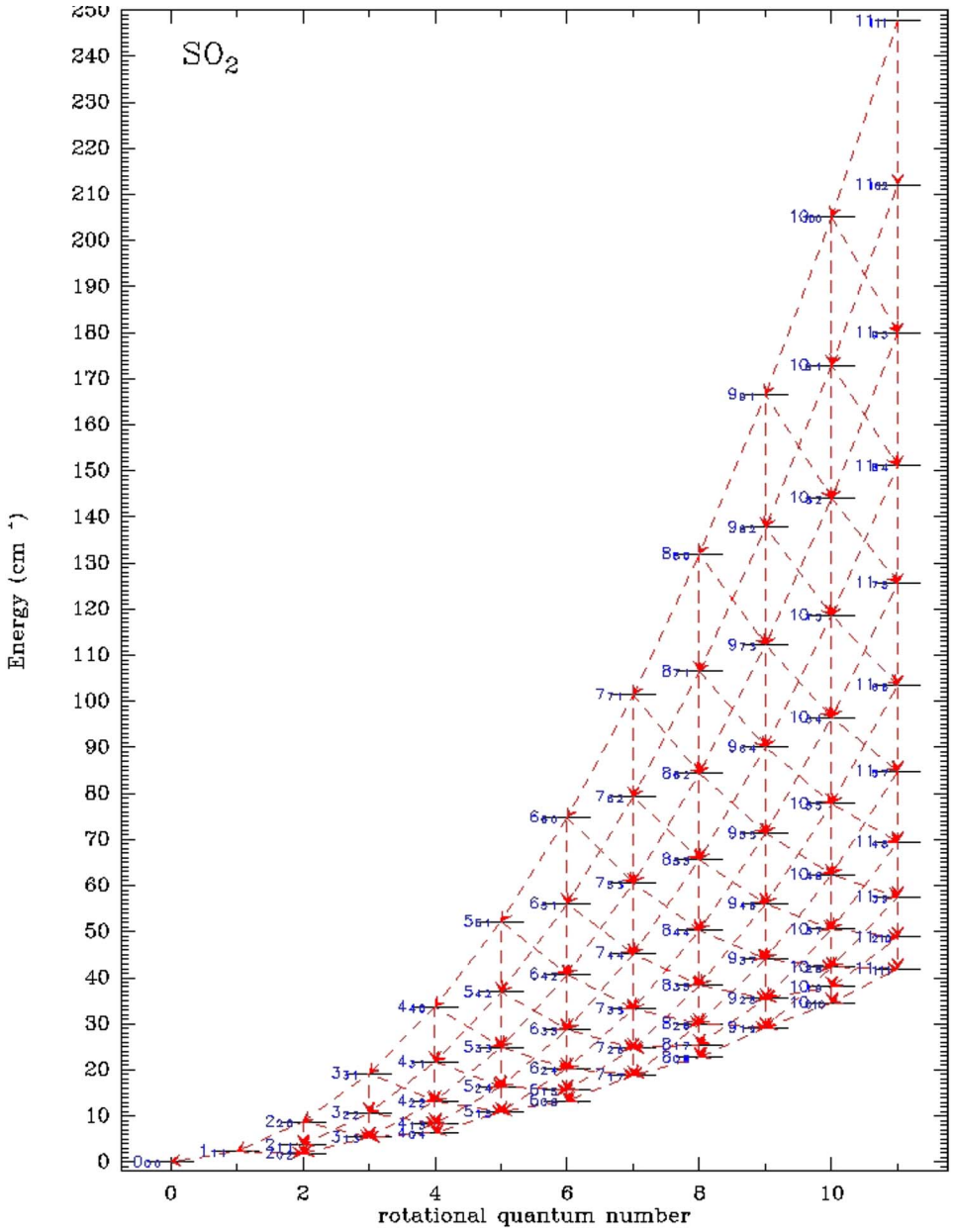

FIG. 3. 31 lowest rotational levels of the SO_2 molecule.

spectroscopic notation, to the *b*-axis. The nuclear spin statistics for the identical oxygen nuclei with spin 0 allows only asymmetric top levels with K_a, K_c either *ee* or *oo*, where *e*/*o* indicates even /odd integer values.[7] The energy of the lowest 31 rotational levels of SO_2 are compared in Table IV to the values given in the JPL catalog[27] and shown in Fig. 3 using the same numbering as in the work of Green.[7]

The calculations were carried out using the hybrid log-derivative Airy propagator of Alexander and Manolopoulos.[28] The various propagation parameters were tested to obtain convergence for the lowest 31 levels and for energies up to 150 cm^{-1}. Typically the minimum and the maximum range was $R_{min}=5$ and $R_{max}=40$ bohrs. The Airy propagation starts from $R=20$ bohrs with an accuracy parameter taken as 0.0003. We increase the MOLSCAT's parameter steps from 10 at the highest energies (≥ 100 cm^{-1}) up to 70 at the lowest energy in order to properly describe the details of the radial function. Only the transitions between the 31 lowest levels were calculated and 72 levels were included in the basis set to obtain convergence better than 5% on the collisional cross sections. The convergence of the cross sections with the total angular momentum J_{tot} was carefully studied. J_{tot} increases gradually from 27 (at low energies) up to 60 at the highest energies (see Table V).

We checked at a total energy $E=E_{coll}+E_{rot}=100$ cm^{-1}, where E_{coll} represents the kinetic energy of the collision and E_{rot} the energy of a given SO_2 rotational level [$E_{rot}(J_2=0)=0$ for H_2], that the inclusion of the $J_2=2$ channel (closed at the considered energies) has small effects on the calculated cross sections (see Fig. 4 for transitions starting from level 5_{42}, number $I=30$).

We carefully spanned the energy range to take into account the presence of resonances. The energy steps were 0.2 cm^{-1} below 50 cm^{-1}, 1.0 cm^{-1} between 50 and 100 cm^{-1}, and 5 cm^{-1} between 100 and 150 cm^{-1}. A linear extrapolation procedure was adopted for energies from 150 up to 300 cm^{-1} in order to obtain fully converged rate coefficients for temperatures up to 30 K.

TABLE V. Table of J_{tot} values.

Energy range (cm^{-1})	J_{tot}
0–20	27
20–30	30
30–32	33
32–35	35
35–40	37
40–70	40
70–79	45
80–115	50
120–135	55
140–150	60

A typical variation of the cross sections with energy is shown in Fig. 5 for the transition $3_{31} \rightarrow 4_{31}$ (transition 16–18 with the adopted numbering). We see that for energies between the threshold and about 60 cm^{-1} above threshold the cross sections display many resonances justifying our very fine energy grid.

These resonances, found in other systems,[8,9,29] are related to the presence of an attractive potential well which allows quasibound states to be formed.[30,31] Quasibound states may arise from tunneling through the centrifugal energy barrier (shape resonances) or they may form through excitation of the molecule to an asymptotically closed channel (Feschbach resonances). Owing to the very small spacing between the SO_2 rotational levels, both types of resonances may be found in the same energy range.

IV. ROTATIONAL INELASTIC RATE COEFFICIENTS

The state-to-state rotational inelastic rates are the Boltzmann thermal average at temperature T of state-to-state inelastic cross sections,

$$R(\beta \rightarrow \beta') = \int_0^\infty \sigma_{\beta \rightarrow \beta'}(E_{coll}) E_{coll} e^{-E_{coll}/kT} dE_{coll}, \qquad (8)$$

where k is the Boltzmann constant, $\beta = J_{K_a,K_c}$, J_2. Rate coefficients obey the detailed balance relation

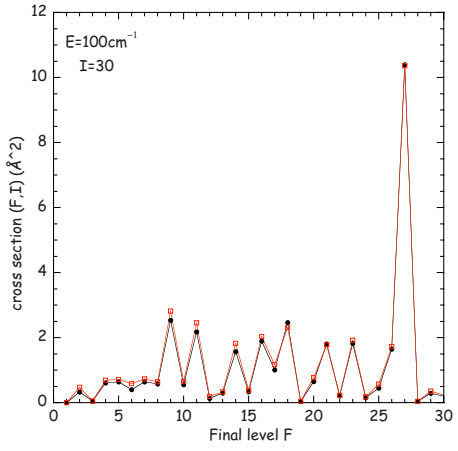

FIG. 4. Comparison between cross sections for SO_2 in collision with para-$H_2(J_2=0,2)$ in red and para-$H_2(J_2=0)$ in black. The total energy is 100 cm^{-1}, the initial level is $J_{K_a,K_c}=5_{4,2}$ (number 30). The final levels are identified through the numbers given in Table IV).

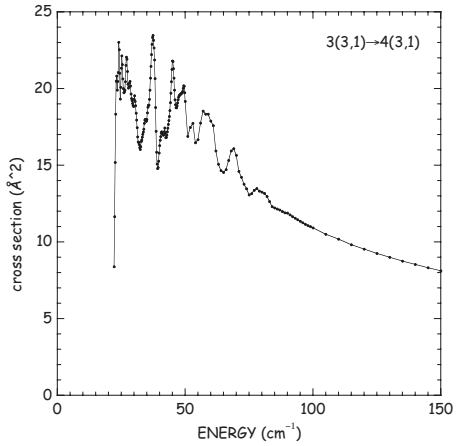

FIG. 5. SO_2–H_2 collisions. Quantum excitation cross section for the transition $3_{31} \rightarrow 4_{31}(I=16 \rightarrow F=18)$ as a function of the energy $E=E_{col}+E_i$ (I and J label the rotational levels as indicated in Table IV).

$$R(\beta' \rightarrow \beta) = \frac{(2J+1)}{(2J'+1)} \exp\left[\frac{E_{\beta'} - E_\beta}{kT}\right] R(\beta \rightarrow \beta'). \qquad (9)$$

Convergence of the integration in Eq. (8) was tested. Calculations up to 150 cm^{-1} with an extrapolation procedure up to 300 cm^{-1} allow us to determine rate coefficients up to 30 K. Results for the transitions between the ten first levels are given in Tables VI and VII. The complete set of the de-excitation rates among all the first 31 levels of SO_2 are available as EPAPS supplementary material.[32] Excitation rates can be obtained from the detailed balance relation, Eq. (9). We observe the temperature dependence of the rates to be weak within a factor 2–3 (see Fig. 6 for transitions $5_{4,2} - 4_{4,0}$, $4_{3,1} - 3_{3,1}$, and $4_{0,4} - 3_{1,3}$). The same trend was found in H_2O–H_2 collisions.[31] Such a flat low temperature dependence reflects the influence of the deep potential well which supports many shape resonances. It should be noted that in most cases rate coefficients for transitions with $\Delta J > 3$ are small.

For comparison purposes, we give in Tables VI and VII the results obtained at 25 K by Green[7] for collisions with He multiplied by 1.39 to correct for the velocity difference between H_2 and He. In Fig. 7, the two sets of 25 K de-excitation rates are plotted for all the transitions starting from the level $5_{4,2}(I=30)$. It appears clearly that the previous results underestimate the rates by large factors, up to 10, in spite of the similarity of the oscillating behavior which reflects the rotational structure of the levels. Such differences, although less pronounced, were found for other systems.[9,33,34] The large differences between the present calculated rates and the results by Green clearly show that, at low temperatures, a good accuracy in both PES calculations and quantum scattering calculations is needed. Such differences in the rate coefficients may have an important impact on the theoretical predictions of SO_2 line emission in cold dark clouds.

In order to find propensity rules for the excitation/de-excitation rates of SO_2, we present in Fig. 8 the excitation and de-excitation rates from one specific level, $J_{K_aK_c}=4_{31}$, at $T=25$ K. This particular level has been chosen in order to display enough other levels connecting to it, hoping that

TABLE VI. Downward rate coefficients of SO_2 in collision with $H_2(J_2=0)$ as a function of the kinetic temperature (in units of $cm^3\ s^{-1}$). For comparison, the IOS results at 25 K, obtained by Green (Ref. 7) for collision with He and multiplied by 1.39 to take into account the mass ratio between He and H_2, are given in the last column.

$I \rightarrow F$	Transition	5 K	10 K	15 K	20 K	25 K	30 K	IOS[a] (25 K)
2–1	$2_{0,2}-0_{0,0}$	4.9480×10^{-11}	4.2460×10^{-11}	4.0840×10^{-11}	4.0550×10^{-11}	4.0550×10^{-11}	4.0590×10^{-11}	1.163×10^{-11}
3–1	$1_{1,1}-0_{0,0}$	3.6720×10^{-11}	2.7280×10^{-11}	2.2200×10^{-11}	1.9160×10^{-11}	1.7230×10^{-11}	1.5960×10^{-11}	3.975×10^{-12}
3–2	$1_{1,1}-2_{0,2}$	9.1720×10^{-11}	7.1610×10^{-11}	6.0760×10^{-11}	5.4010×10^{-11}	4.9400×10^{-11}	4.6050×10^{-11}	5.921×10^{-12}
4–1	$2_{1,1}-0_{0,0}$	9.9050×10^{-12}	6.4340×10^{-12}	4.7470×10^{-12}	3.7250×10^{-12}	3.0390×10^{-12}	2.5470×10^{-12}	$0.000\times10^{+00}$
4–2	$2_{1,1}-2_{0,2}$	8.2530×10^{-11}	6.3110×10^{-11}	5.3020×10^{-11}	4.6930×10^{-11}	4.2950×10^{-11}	4.0220×10^{-11}	7.812×10^{-12}
4–3	$2_{1,1}-1_{1,1}$	9.9700×10^{-11}	9.4820×10^{-11}	9.4460×10^{-11}	9.5140×10^{-11}	9.5770×10^{-11}	9.6120×10^{-11}	2.210×10^{-11}
5–1	$3_{1,3}-0_{0,0}$	2.3470×10^{-11}	1.9450×10^{-11}	1.7580×10^{-11}	1.6460×10^{-11}	1.5670×10^{-11}	1.5050×10^{-11}	1.904×10^{-12}
5–2	$3_{1,3}-2_{0,2}$	6.9670×10^{-11}	5.7630×10^{-11}	5.0750×10^{-11}	4.6500×10^{-11}	4.3720×10^{-11}	4.1820×10^{-11}	7.242×10^{-12}
5–3	$3_{1,3}-1_{1,1}$	3.8000×10^{-11}	3.5110×10^{-11}	3.3960×10^{-11}	3.3430×10^{-11}	3.3110×10^{-11}	3.2870×10^{-11}	9.271×10^{-12}
5–4	$3_{1,3}-2_{1,1}$	4.8420×10^{-11}	4.2930×10^{-11}	4.0300×10^{-11}	3.8750×10^{-11}	3.7720×10^{-11}	3.7010×10^{-11}	8.632×10^{-12}
6–1	$4_{0,4}-0_{0,0}$	1.0400×10^{-11}	8.5910×10^{-12}	8.0280×10^{-12}	7.8860×10^{-12}	7.9050×10^{-12}	7.9910×10^{-12}	1.432×10^{-12}
6–2	$4_{0,4}-2_{0,2}$	7.7470×10^{-11}	7.0740×10^{-11}	6.8740×10^{-11}	6.8460×10^{-11}	6.8720×10^{-11}	6.9120×10^{-11}	1.876×10^{-11}
6–3	$4_{0,4}-1_{1,1}$	2.4810×10^{-11}	2.1470×10^{-11}	1.9550×10^{-11}	1.8350×10^{-11}	1.7540×10^{-11}	1.6950×10^{-11}	2.238×10^{-12}
6–4	$4_{0,4}-2_{1,1}$	4.9430×10^{-11}	4.1100×10^{-11}	3.7000×10^{-11}	3.4530×10^{-11}	3.2850×10^{-11}	3.1610×10^{-11}	4.087×10^{-12}
6–5	$4_{0,4}-3_{1,3}$	4.8330×10^{-11}	3.8960×10^{-11}	3.2320×10^{-11}	2.7890×10^{-11}	2.4860×10^{-11}	2.2730×10^{-11}	3.572×10^{-12}
7–1	$4_{1,3}-0_{0,0}$	3.6950×10^{-12}	2.5220×10^{-12}	1.8800×10^{-12}	1.4820×10^{-12}	1.2120×10^{-12}	1.0170×10^{-12}	$0.000\times10^{+00}$
7–2	$4_{1,3}-2_{0,2}$	3.1400×10^{-11}	2.3910×10^{-11}	1.9640×10^{-11}	1.6990×10^{-11}	1.5190×10^{-11}	1.3890×10^{-11}	1.169×10^{-12}
7–3	$4_{1,3}-1_{1,1}$	2.3710×10^{-11}	2.2940×10^{-11}	2.2820×10^{-11}	2.3060×10^{-11}	2.3430×10^{-11}	2.3830×10^{-11}	3.864×10^{-12}
7–4	$4_{1,3}-2_{1,1}$	6.9780×10^{-11}	6.6080×10^{-11}	6.5240×10^{-11}	6.5310×10^{-11}	6.5600×10^{-11}	6.5890×10^{-11}	1.626×10^{-11}
7–5	$4_{1,3}-3_{1,3}$	6.7680×10^{-11}	6.3970×10^{-11}	6.2660×10^{-11}	6.2280×10^{-11}	6.2170×10^{-11}	6.2140×10^{-11}	1.077×10^{-11}
7–6	$4_{1,3}-4_{0,4}$	6.6920×10^{-11}	6.0250×10^{-11}	5.4370×10^{-11}	5.0360×10^{-11}	4.7610×10^{-11}	4.5720×10^{-11}	9.257×10^{-12}
8–1	$2_{2,0}-0_{0,0}$	2.0600×10^{-11}	1.9380×10^{-11}	1.8950×10^{-11}	1.8700×10^{-11}	1.8510×10^{-11}	1.8330×10^{-11}	1.626×10^{-12}
8–2	$2_{2,0}-2_{0,2}$	5.4150×10^{-11}	4.6220×10^{-11}	4.2300×10^{-11}	3.9790×10^{-11}	3.7970×10^{-11}	3.6550×10^{-11}	2.488×10^{-12}
8–3	$2_{2,0}-1_{1,1}$	2.7220×10^{-11}	2.5200×10^{-11}	2.3650×10^{-11}	2.2540×10^{-11}	2.1790×10^{-11}	2.1300×10^{-11}	4.337×10^{-12}
8–4	$2_{2,0}-2_{1,1}$	3.3320×10^{-11}	2.9230×10^{-11}	2.5380×10^{-11}	2.2520×10^{-11}	2.0430×10^{-11}	1.8910×10^{-11}	3.155×10^{-12}
8–5	$2_{2,0}-3_{1,3}$	5.5350×10^{-11}	4.8960×10^{-11}	4.5090×10^{-11}	4.2440×10^{-11}	4.0480×10^{-11}	3.8970×10^{-11}	4.059×10^{-12}
8–6	$2_{2,0}-4_{0,4}$	3.6580×10^{-11}	3.0680×10^{-11}	2.7010×10^{-11}	2.4560×10^{-11}	2.2790×10^{-11}	2.1450×10^{-11}	1.150×10^{-12}
8–7	$2_{2,0}-4_{1,3}$	3.9780×10^{-11}	3.6340×10^{-11}	3.3470×10^{-11}	3.1330×10^{-11}	2.9670×10^{-11}	2.8360×10^{-11}	3.711×10^{-12}

[a]Reference 7.

TABLE VII. Downward rate coefficients of SO_2 in collision with $H_2(J_2=0)$ as a function of the kinetic temperature (in units of $cm^3\ s^{-1}$). For comparison, the IOS results at 25 K, obtained by Green (Ref. 7) for collision with He and multiplied by 1.39 to take into account the mass ratio between He and H_2, are given in the last column.

$I \rightarrow F$	transition	5 K	10 K	15 K	20 K	25 K	30 K	IOS[a] (25 K)
9–1	$3_{2,2}-0_{0,0}$	3.0670×10^{-12}	2.7230×10^{-12}	2.4380×10^{-12}	2.1870×10^{-12}	1.9680×10^{-12}	1.7780×10^{-12}	$0.000\times10^{+00}$
9–2	$3_{2,2}-2_{0,2}$	4.6280×10^{-11}	4.4580×10^{-11}	4.3520×10^{-11}	4.2760×10^{-11}	4.2130×10^{-11}	4.1570×10^{-11}	3.489×10^{-12}
9–3	$3_{2,2}-1_{1,1}$	1.5230×10^{-11}	1.3940×10^{-11}	1.2480×10^{-11}	1.1240×10^{-11}	1.0260×10^{-11}	9.4800×10^{-12}	9.647×10^{-13}
9–4	$3_{2,2}-2_{1,1}$	4.2180×10^{-11}	4.0060×10^{-11}	3.7720×10^{-11}	3.5980×10^{-11}	3.4710×10^{-11}	3.3780×10^{-11}	5.365×10^{-12}
9–5	$3_{2,2}-3_{1,3}$	3.1540×10^{-11}	2.8780×10^{-11}	2.6530×10^{-11}	2.4930×10^{-11}	2.3840×10^{-11}	2.3130×10^{-11}	3.864×10^{-12}
9–6	$3_{2,2}-4_{0,4}$	4.7030×10^{-11}	3.8640×10^{-11}	3.3900×10^{-11}	3.0860×10^{-11}	2.8720×10^{-11}	2.7150×10^{-11}	1.737×10^{-12}
9–7	$3_{2,2}-4_{1,3}$	3.9930×10^{-11}	3.3950×10^{-11}	2.9960×10^{-11}	2.7170×10^{-11}	2.5170×10^{-11}	2.3720×10^{-11}	3.100×10^{-12}
9–8	$3_{2,2}-2_{2,0}$	6.4360×10^{-11}	6.5640×10^{-11}	6.8170×10^{-11}	7.0370×10^{-11}	7.1960×10^{-11}	7.3040×10^{-11}	2.168×10^{-11}
10–1	$5_{1,5}-0_{0,0}$	7.7060×10^{-12}	7.4870×10^{-12}	7.3420×10^{-12}	7.2610×10^{-12}	7.2230×10^{-12}	7.2160×10^{-12}	1.129×10^{-12}
10–2	$5_{1,5}-2_{0,2}$	3.8070×10^{-11}	3.5040×10^{-11}	3.3170×10^{-11}	3.1870×10^{-11}	3.0910×10^{-11}	3.0160×10^{-11}	4.420×10^{-12}
10–3	$5_{1,5}-1_{1,1}$	1.0190×10^{-11}	8.0810×10^{-12}	7.0360×10^{-12}	6.4440×10^{-12}	6.0860×10^{-12}	5.8610×10^{-12}	8.354×10^{-13}
10–4	$5_{1,5}-2_{1,1}$	1.5600×10^{-11}	1.2690×10^{-11}	1.0830×10^{-11}	9.5950×10^{-12}	8.7400×10^{-12}	8.1320×10^{-12}	6.769×10^{-13}
10–5	$5_{1,5}-3_{1,3}$	5.0970×10^{-11}	5.0290×10^{-11}	5.0470×10^{-11}	5.1080×10^{-11}	5.1760×10^{-11}	5.2380×10^{-11}	1.585×10^{-11}
10–6	$5_{1,5}-4_{0,4}$	5.1470×10^{-11}	4.4130×10^{-11}	3.8410×10^{-11}	3.4430×10^{-11}	3.1650×10^{-11}	2.9690×10^{-11}	5.240×10^{-12}
10–7	$5_{1,5}-4_{1,3}$	4.3450×10^{-11}	3.5800×10^{-11}	3.1280×10^{-11}	2.8340×10^{-11}	2.6300×10^{-11}	2.4830×10^{-11}	3.544×10^{-12}
10–8	$5_{1,5}-2_{2,0}$	1.6330×10^{-11}	1.4600×10^{-11}	1.3500×10^{-11}	1.2760×10^{-11}	1.2250×10^{-11}	1.1900×10^{-11}	1.245×10^{-12}
10–9	$5_{1,5}-3_{2,2}$	2.4030×10^{-11}	2.2490×10^{-11}	2.0890×10^{-11}	1.9610×10^{-11}	1.8590×10^{-11}	1.7770×10^{-11}	1.904×10^{-12}

[a]Reference 7.

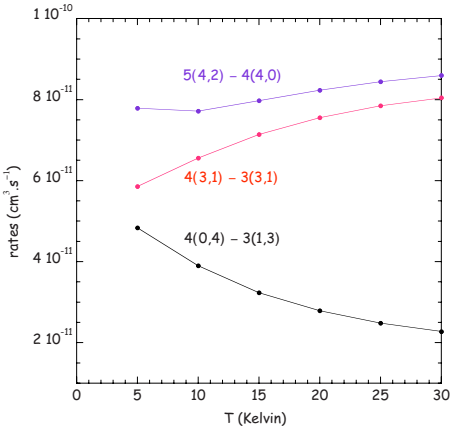

FIG. 6. Collisional rate coefficients for rotational de-excitation of SO_2 as function of temperature.

some pattern would emerge from the various computed rates. The three most important rates are those that connect the initial level with the same value of $K_a=3$ and $\Delta K_c=0,+2$, along with $\Delta J=\pm 1,+2$. The following family of connected levels are those with $\Delta K_a=-1$ (and also to a lesser extent $\Delta K_a=+1$). Then comes the larger difference in $\Delta K_a<-1$, and eventually the families of levels with the same value of J, but with decreasing values of K_a.

The propensity rules are thus somewhat different from those obtained for the H_2O-H_2 or H_2CO-H_2 collisions.[35,36] Here, because of the vastly different values of $I_a \ll I_b \sim I_c$, the mechanical reorientation of the angular momentum with respect to the a axis, given by the K_a value, is the most difficult. The largest rates are those with minimal ΔK_a, with K_c and J values changing according to the limitations of the allowed quantum numbers. In the same spirit, the second noticeable effect is the monotonic decrease in the collision rate for a given value of J, as $|\Delta K_a|$ increases, corresponding to a simple reorientation of the angular momentum vector $\boldsymbol{J}$. The final rule is that pure energy considerations seem minor, if they do not take into account the angular momentum vector orientation, even at these low temperatures, in accordance with what some of us have observed for water.[35] This is best seen in the apparently random shape of Fig. 7, where the rotational levels are ordered only with respect to their eigenenergies.

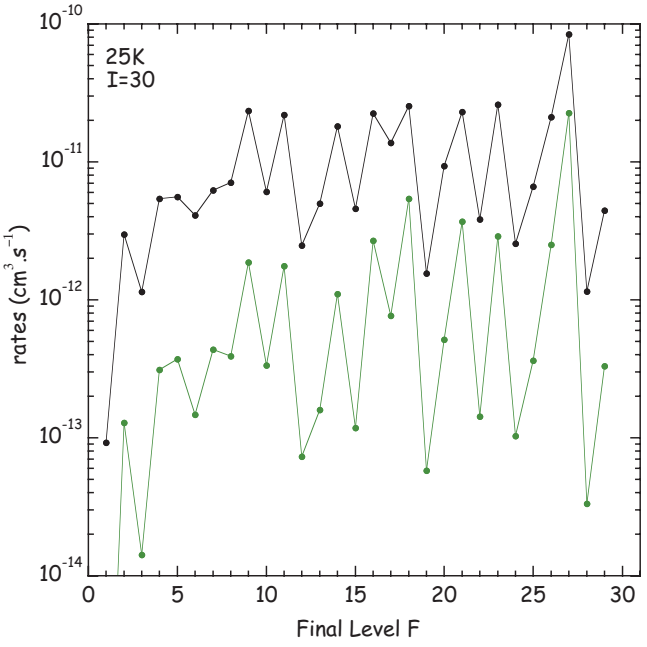

FIG. 7. Downward rate coefficients for SO_2 in collision with para-H_2 from level $5_{4,2}(I=30)$ at 25 K. Present quantum calculations in black. For comparison IOS collisional de-excitation rate coefficients from Green (Ref. 7) in green.

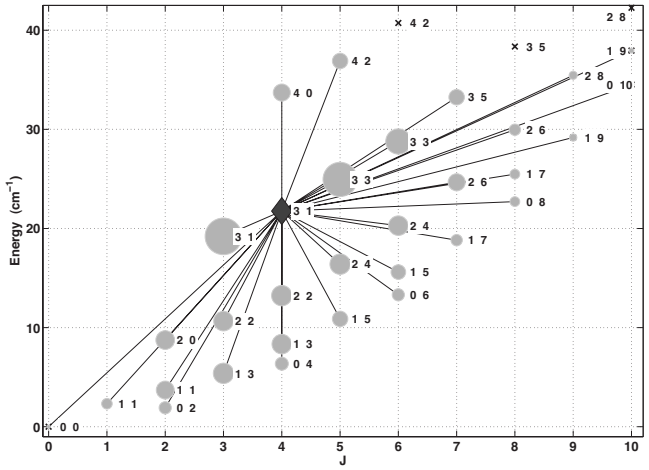

FIG. 8. Levels connected to the initial level 4_{31} level, denoted by a black diamond, by a noticeable excitation ($\geq 10^{-12}$ cm^3 s^{-1}) or de-excitation rate, at 25 K. Crosses correspond to rates below the threshold. The *area* of each gray disk is proportional to the rate. Each level is denoted by its J value, on the x-axis, its energy, on the y-axis, and the values of K_a, K_c. Note that selection rules preclude the existence of many levels.

V. CONCLUSION

We have presented in this paper a rigid rotor study of the interaction between sulfur dioxide and hydrogen molecules. Calculation was performed at the CCSD(T) level of theory with thoroughly selected basis set. The potential fit and the corresponding angular expansion suitable for close-coupling scattering calculations were estimated to be accurate within 1 cm^{-1}.

We have computed state-to-state rate coefficients between the first 31 rotational levels for collisions with para $H_2(J_2=0)$ and temperatures up to 30 K. Preliminary results show that inclusion of the $H_2(J_2=2)$ level is of minor consequence at the considered temperatures. Large differences with the scaled SO_2-He rates by Green[7] are observed with expected consequences on the modeling of dense molecular clouds. A propensity rule that favors $J_{K_aK_c}-J'_{K'_aK'_c}$ transitions with $|\Delta K_a|=0$ is found. This trend may be assigned to the difficulty to reorientate the angular momentum vector with respect to the a axis.

We stress that, due to the increasingly large computer time and memory ressources needed for these calculations, extension of full close-coupling calculations to high-J levels and temperatures is not realistic presently. The QCT method seems to be an alternative to investigate very high rotational levels.[35] Such calculations will be considered in future works as well as calculations of rate coefficients for collisions with ortho-H_2 at both low and higher temperatures.

ACKNOWLEDGMENTS

The calculations of *ab initio* PES were performed at the Centro de Supercomputación de Galicia, CESGA, and on the parallel machine MPOPM of Paris Observatory. The scattering calculations were performed at the IDRIS-CNRS French National Computing Center (Institut de Développement et des Ressources en Informatique Scientifique du Centre National de la Recherche Scientifique) under Project No. 060883 and on local work stations of the Centre Informatique of Paris Observatory. L.C.-V. was supported in 2006-2008 by the FP6 Research Training Network "Molecular Universe" under Contract No. MCRTN-CT-2004-512302 and in 2008-2009 by a grant of the Lavoisier Program of the french Foreign Office Ministry. M.-L. Senent acknowledges the MEC (Spain) for the Grant No. AYA2005-00702. We would like to acknowledge J. Cernicharo for his continuing interest in this work and for fruitful discussions.

The authors wish to acknowledge their friend and colleague Pierre Valiron who actively participated to the work that lead to this paper. Pierre passed away on 31th August 2008, and he is deeply missed.

[1] L. E. Snyder, J. M. Hollis, B. L. Ulich, F. L. Lovas, D. R. Johnson, and D. Buhl, Astrophys. J. **198**, L81 (1975).
[2] W. M. Irvine, J. C. Good, and F. P. Schloerb, Astron. Astrophys. **127**, L10 (1983).
[3] J. E. Dickens, W. M. Irvine, R. L. Snell, E. A. Bergin, F. P. Schloerb, P. Pratap, and M. P. Miralles, Astrophys. J. **542**, 870 (2000).
[4] F. Lique, A. Spielfiedel, and J. Cernicharo, Astron. Astrophys. **451**, 1125 (2006).
[5] F. Lique, J. Cernicharo and P. Cox, Astrophys. J. **653**, 1342 (2006).
[6] F. Daniel, J. Cernicharo, and M.-L. Dubernet, Astrophys. J. **648**, 461 (2006).
[7] S. Green, Astrophys. J., Suppl. **100**, 213 (1995).
[8] F. Lique, M.-L. Senent, A. Spielfiedel, and N. Feautrier, J. Chem. Phys. **126**, 164312 (2007).
[9] M. Wernli, L. Wiesenfeld, A. Faure and P. Valiron, Astron. Astrophys. **464**, 1147 (2007); Astron. Astrophys. **475**, 391 (2007).
[10] J. Klos and F. Lique, Mon. Not. R. Astron. Soc. **390**, 239 (2008).
[11] P. Jankowski and K. Szalewicz, J. Chem. Phys. **123**, 104301 (2005).
[12] A. Faure, P. Valiron, M. Wernli, L. Wiesenfeld, C. Rist, J. Noga, and J. Tennyson, J. Chem. Phys. **122**, 221102 (2005).
[13] P. Valiron, M. Wernli, A. Faure, L. Wiesenfeld, C. Rist, S. Kedzuch, and J. Noga, J. Chem. Phys. **129**, 134306 (2008).
[14] F. J. Lovas, J. Phys. Chem. Ref. Data **7**, 1445 (1978).
[15] T. R. Phillips, S. Maluendes, A. D. McLean, and S. Green, J. Chem. Phys. **101**, 5824 (1994).
[16] S. Green, J. Chem. Phys. **103**, 1035 (1995).
[17] P. J. Knowles, C. Hampel, and H.-J. Werner, J. Chem. Phys. **99**, 5219 (1993).
[18] P. J. Knowles, C. Hampel, and H.-J. Werner, J. Chem. Phys. **112**, 3106 (2000).
[19] MOLPRO is a package of ab initio programs written by H.-J. Werner and P. J. Knowles, with contributions from J. Almlöf, R. D. Amos, M. J. Deegan, S. T. Elbert,C. Hampel, W. Meyer, K. Peterson, R. Pitzer, A. J. Stone, P. R. Taylor, R. Lindh M. E. Mura, and T. Thorsteisson.
[20] S. F. Boys and F. Bernardi, Mol. Phys. **19**, 553 (1970).
[21] D. E. Woon and T. H. Dunning, Jr., J. Chem. Phys. **100**, 2975 (1994).
[22] H. L. Williams, E. M. Mas, K. Szalewicz, and B. Jeziorski, J. Chem. Phys. **103**, 7374 (1995).
[23] O. Akin-Ojo, R. Bukowski, and K. Szalewicz, J. Chem. Phys. **119**, 8379 (2003).
[24] T. R. Phillips, S. Maluendes, and S. Green, J. Chem. Phys. **102**, 6024 (1995).
[25] P. Valiron and G. C. McBane, program repository on: http://www-laog.obs.ujf-grenoble.fr/valiron/molscat/).
[26] J. M. Hutson and S. Green, MOLSCAT computer code, version 14 (1994) (distributed by Collaborative Computational Project No. O of the Engineering and Physical Sciences Research Council UK)
[27] J. P. L. Molecular Spectroscopy Catalog, http://spec.jpl.nasa.gov/ftp/pub/catalog/c064002.cat.
[28] M. H. Alexander and D. E. Manolopoulos, J. Chem. Phys. **86**, 2044 (1987).
[29] M.-L. Dubernet and A. Grosjean, Astron. Astrophys. **390**, 793 (2002).
[30] L. N. Smith, D. J. Malik, and D. Secrest, J. Chem. Phys. **71**, 4502 (1979).
[31] K. M. Christoffel and J. M. Bowman, J. Chem. Phys. **78**, 3952 (1983).
[32] See EPAPS supplementary material at 10.1063/1.3158357 E-JCPSA6-131-006926 for a complete set of the deexcitation rates among the first 31 levels of SO_2. For more information on EPAPS, see http://www.aip.org/pubservs/epaps.html.
[33] F. Lique, R. Tobola, J. Klos, N. Feautrier, A. Spielfiedel, L. F. M. Vincent, G. Chalasiński, and M. H. Alexander, Astron. Astrophys. **478**, 567 (2008).
[34] T. R. Phillips, S. Maluendes, and S. Green, Astrophys. J. Suppl. Ser. **107**, 467 (1996).
[35] A. Faure, N. Crimier, C. Ceccarelli, P. Valiron, L. Wiesenfeld, and M.-L. Dubernet, Astron. Astrophys. **472**, 1029 (2007).
[36] N. Troscompt, A. Faure, L. Wiesenfeld, C. Ceccarelli, and P. Valiron, Astron. Astrophys. **493**, 687 (2009).